Inorganic Chemistry

Article

pubs.acs.org/IC

Reversible Solvatomagnetic Effect in Novel Tetranuclear Cubane-Type Ni_4 Complexes and Magnetostructural Correlations for the $[Ni_4(\mu_3\text{-}O)_4]$ Core

Animesh Das, Felix J. Klinke, Serhiy Demeshko, Steffen Meyer, Sebastian Dechert, and Franc Meyer*

Institute of Inorganic Chemistry, Georg-August-University, Tammannstrasse 4, D-37077 Göttingen, Germany

Supporting Information

ABSTRACT: A new family of tetranuclear nickel cube complexes $[Ni_4L_4(solv)_4]$ (**1**, solv = MeOH; **2**, solv = H_2O; H_2L = pyrazole-based tridentate {ONO} ligand) has been studied in detail, in particular by X-ray diffraction and superconducting quantum interference device (SQUID) magnetometry. Different solvates **1·H$_2$O**, **2·4C$_3$H$_6$O**, **2·CH$_2$Cl$_2$**, and **2·H$_2$O** were obtained in crystalline form. Only small structural variations were found for the Ni−O−Ni angles of the $[Ni_4O_4]$ cores of those compounds, but these slight variations have dramatic consequences for the magnetic properties. $[Ni_4L_4(MeOH)_4]\cdot H_2O$ (**1·H$_2$O**) and $[Ni_4L_4(H_2O)_4]\cdot H_2O$ (**2·H$_2$O**) can be reversibly interconverted in the solid state by exposure to the respective solvent, MeOH or H_2O, and this goes along with a switching of the spin ground state from magnetic ($S_T = 4$) to diamagnetic ($S_T = 0$). Likewise the (irreversible) loss of lattice solvent in $[Ni_4L_4(H_2O)_4]\cdot 4C_3H_6O$ (**2·4C$_3$H$_6$O**) to give **2·2C$_3$H$_6$O** changes the ground state from $S_T = 4$ to $S_T = 0$. In view of these dramatic solvatomagnetic effects for the present $[Ni_4L_4(solv)_4]$ complexes, which occur upon extrusion of lattice solvent or facile exchange of coordinated solvent molecules while keeping the robust $[Ni_4O_4]$ core intact, a note of care is issued: whenever magnetic data are obtained for powdered material or for crystals that easily loose lattice solvent molecules, the magnetic properties may not necessarily reflect the situation observed in the corresponding single crystal diffraction study. Finally, a thorough analysis of the present series of complexes as well as other $\{Ni_4(\mu_3\text{-}OR)_4\}$ cubes reported in the literature confirms that a correlation between the $(Ni-O-Ni)_{av}$ bond angle and J in $[Ni_4O_4]$ cubane complexes does indeed exist.

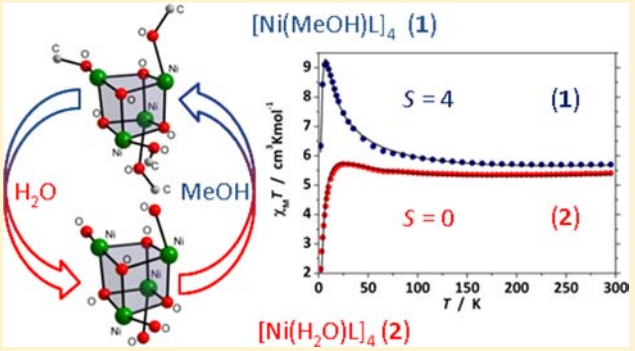

INTRODUCTION

Combining magnetic responses with some other chemical or physicochemical properties of materials is one of the most fascinating aspects in the field of molecular magnetism. In 1999 Kahn introduced the term *molecular magnetic sponges* (MMS) for a class of molecule-based materials that reversibly switch from a nonmagnetic to a magnetically ordered state through a simple chemical process such as dehydration−rehydration.[1] Ochkoshi, Hashimoto et al. in 2003 coined the term *solvatomagnetic effect* (SME) to denote the solvent modulation of magnetic properties of cobalt hexacyanochromate-based magnets that result from the exchange of coordinated water molecules by ethanol molecules.[2] Actually both terms are often used synonymously for characterizing magnetic sponge-like behavior,[3] while the term SME is also used in a more general sense to describe the effect of exchange[2] or release[4] of solvent molecules on magnetic properties. However, for crystalline material some authors are not using any of these terms but prefer to describe magnetic sponge-like behavior as reversible sorption−desorption *single-crystal-to-single-crystal transformations* (SCSC).[5]

While compounds showing SME are molecule-based, most of them are either coordination polymers or even metal organic frameworks (MOFs), or their structural dimensionality changes, for example, from initial zero-dimensional (0D) to three-dimensional (3D) upon solvent influence.[6] In fact, the switching of magnetic properties by sorption/desorption of solvent guest molecules in MOFs is an active field of research with interesting prospects.[7] However, there are only few examples of SMEs where the systems are truly molecular, such as (i) a dinuclear Dy^{III}-based *single molecule magnet* (SMM),[8] (ii) a dinuclear fluorous Cu^{II} carboxylate complex,[9] and (iii) a tetranuclear Ni^{II} azido-bridged complex from our lab.[10] The latter two compounds show irreversible[10] or only partially reversible[9b] SME. Furthermore, the dehydration step of the SME usually requires heating to high temperatures and/or the presence of a drying agent, for example, the above-mentioned Dy^{III}-SMM has to be heated to 433 K under reduced pressure to obtain the dehydrated phase.[8] It should be noted here that closely related approaches deal with the investigation of solvent-dependent spin-crossover systems,[11] which are not included in the present discussion.

Received: March 12, 2012
Published: July 23, 2012

   dx.doi.org/10.1021/ic300535d | Inorg. Chem. 2012, 51, 8141−8149

In this work we report a tetranuclear cube-like complex $[Ni_4L_4(MeOH)_4]\cdot H_2O$ (**1·H$_2$O**) that shows a pronounced solvatomagnetic effect, namely, a switching of the spin ground state at ambient temperature induced by the exchange of coordinated solvent molecules (MeOH versus H_2O). Several solvates of this new type of Ni_4 cubane have been characterized crystallographically and thoroughly investigated to rationalize the findings. Transition metal complexes with a cubane $\{M_4X_4\}$ core are quite prominent in modern coordination chemistry. Sulfido-bridged Fe-cubes have been extensively studied as models for Fe/S protein cofactors,[12] and $\{Mn_4O_4\}$ as well as $\{Co_4O_4\}$ cubane clusters are attracting much attention as bioinspired water oxidation catalysts.[13] Since $\{M_4X_4\}$ cubes may have high-spin ground states because of accidental orthogonality of magnetic orbitals, they have also become an important class of oligonuclear complexes in the field of molecular magnetism.[14] Specifically, the search for tetranuclear nickel(II) complexes with a cubane-type $\{Ni_4O_4\}$ core has been fired by the discovery that this motif can give rise to SMM behavior.[15−17]

RESULTS AND DISCUSSION

Synthesis and Structural Characterization of Complexes. The pyrazole based tridentate diol ligand H_2L (Scheme 1) has been chosen as a flexible and potentially bridging ligand for this work. We recently used H_2L for the synthesis of a family of heterometallic $\{Mn^{III}_2Ni^{II}_3\}$ SMMs that have an S_T = 7 ground state. H_2L, in its singly deprotonated form, was shown to mediate ferromagnetic exchange between the metal ions of those quasi-linear $\{Mn^{III}_2Ni^{II}_3\}$ SMMs because of accidental orthogonality of the magnetic orbitals.[18] We now employed this ligand in combination with only one of the metal ions used for the above heterometallic SMMs, namely, with nickel(II), to obtain a new series of $\{Ni_4(\mu_3\text{-}O)_4\}$ cubane core structures (Scheme 1).

Scheme 1. Overview of the Synthesis and Topology of 1 and 2[a]

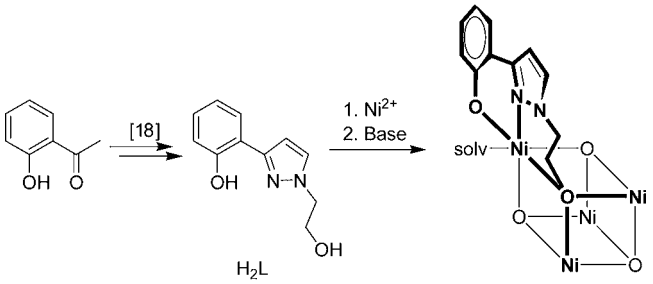

[a]For clarity only one ligand and its coordination mode (bold) at the $\{Ni_4(\mu_3\text{-}O)_4\}$ core are shown.

Treatment of a methanolic solution of H_2L with 1 equiv of $Ni(OAc)_2\cdot 4H_2O$ and 2 equiv of NaOH lead to rapid precipitation of a dark green solid, which could be recrystallized by layering a CH_2Cl_2 solution of the crude material with *n*-hexane, affording large green crystals of **1·H$_2$O**. Following the same procedure, but using moist solvents, crystals of **2·CH$_2$Cl$_2$** and **2·H$_2$O** were obtained. When the dark green precipitate was dissolved in acetone instead of CH_2Cl_2 and the solution left for slow evaporation, crystals of **2·4C$_3$H$_6$O** gradually formed.

Since thorough investigation and interpretation of the magnetic properties of any material requires high purity samples and preferably some structural information, crystalline material was used for all further studies. The molecular structures of $[Ni_4L_4(MeOH)_4]\cdot H_2O$ (**1·H$_2$O**) and $[Ni_4L_4(H_2O)_4]\cdot 4C_3H_6O$ (**2·4C$_3$H$_6$O**), determined by X-ray crystallography, are shown in Figure 1 (see Supporting Information, Figure S1a, for the structure of **2·CH$_2$Cl$_2$**). Selected interatomic distances and angles are given in the Supporting Information. Eight alternately arranged oxygen and metal atoms form a distorted $\{Ni_4O_4\}$ cube with local S_4-symmetry. In case of **1·H$_2$O** this point group is also reflected in the space group $I4_1/a$. In **2·4C$_3$H$_6$O** the symmetry is reduced to C_2, and **2·CH$_2$Cl$_2$** has no crystallographically imposed molecular symmetry. The asymmetric unit of **1·H$_2$O** contains one-fourth of the molecular structure, one-half is present in **2·4C$_3$H$_6$O**, and **2·CH$_2$Cl$_2$** contains two crystallographically independent molecules. Every metal atom is further coordi-

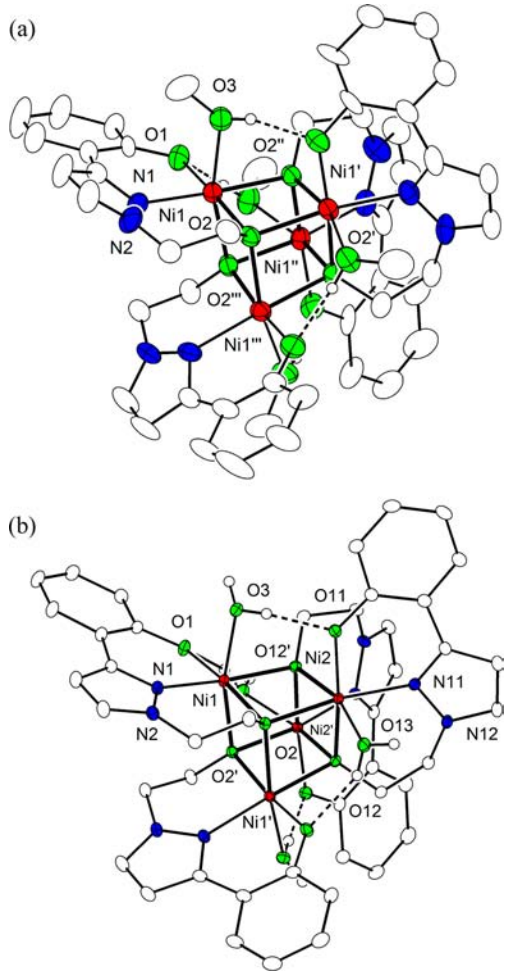

Figure 1. ORTEP plots (30% probability thermal ellipsoids) of the molecular structures of $[Ni_4L_4(MeOH)_4]$ (**1·H$_2$O**) (a) and $[Ni_4L_4(H_2O)_4]$ (**2·4C$_3$H$_6$O**) (b). Most hydrogen atoms and all solvent molecules have been omitted. Symmetry operations used to generate equivalent atoms of **1·H$_2$O**: (′) 1.25−*y*, 0.25+*x*, 1.25−*z*; (″) −0.25+*y*, 1.25−*x*, 1.25−*z*; (‴) 1−*x*, 1.5−*y*, *z*. Symmetry operation used to generate equivalent atoms of **2·4C$_3$H$_6$O**: (′) 1−*x*, *y*, 0.5−*z*.

dx.doi.org/10.1021/ic300535d | *Inorg. Chem.* 2012, 51, 8141−8149

nated by a methanol ligand in case of **1** or a water ligand in case of **2**. The coordination number for all metal atoms is six, which results in a distorted octahedral coordination polyhedron. Three corners of the octahedron are occupied by the O-atoms from the ethoxy arms of three ligands L^{2-}, which act as bridges to the remaining metal atoms within the cubane core. Further positions are occupied by an O-atom from the phenolate part of the ligand, the pyrazole-N of the ligand and one O-atom of the exogenous solvent molecule (MeOH in **1** or H_2O in **2**). Several related complexes with a cube-like $\{Ni_4O_4\}$ core have been previously reported; most similar are nickel(II) complexes containing tridentate 2-(salicylideneamino)ethanol ligands.[19] An interesting feature of all present complexes is the stabilization of the cubane core by hydrogen bonds between the exogenous MeOH or H_2O molecules, which act as hydrogen bond donors, and the phenolate-O, which act as hydrogen bond acceptors (Figure 1 and Supporting Information, Figure S2, Table S7). Thereby four of the six faces (four side faces, **SF**) of the $\{Ni_4O_4\}$ cube are spanned by hydrogen bonds, resulting in somewhat different bond lengths and angles for the involved atoms (Table 1 and Supporting Information, Table S7) compared to those at the two remaining faces at opposite sides of the cube (**OF**). These differences, primarily in the bridging Ni−O−Ni angles (Table 1), are crucial factors that determine the sign of the magnetic exchange interactions through O-atom bridges; their modulation has drastic effects on the ground state of the complexes, as will be shown below.

Table 1. Ni−O−Ni Angles (deg) for $1\cdot H_2O$, $2\cdot 4C_3H_6O$, and $2\cdot CH_2Cl_2$[a]

M−O−M	$1\cdot H_2O$	$2\cdot 4C_3H_6O$	$2\cdot CH_2Cl_2$
$M_A-O_A-M_B$	97.95(4)	97.27(6)	97.7(2)/96.9(2)
$M_A-O_C-M_B$	95.09(4)	94.97(5)	95.1(2)/94.6(2)
$M_A-O_C-M_C$	97.95(4)	98.74(6)	98.6(2)/98.3(2)
$M_A-O_D-M_C$	95.09(4)	94.62(5)	94.4(2)/94.3(2)
$M_A-O_A-M_D$	100.22(4)	100.66(6)	100.3(2)/99.4(2)
$M_A-O_D-M_D$	100.22(4)	100.66(6)	99.1(2)/99.4(2)
$M_B-O_B-M_C$	100.22(4)	99.90(6)	100.3(2)/100.9(2)
$M_B-O_C-M_C$	100.22(4)	99.90(6)	100.0(2)/99.6(2)
$M_B-O_A-M_D$	95.09(4)	94.62(5)	95.1(2)/94.8(2)
$M_B-O_B-M_D$	97.95(4)	98.74(6)	96.8(2)/98.4(2)
$M_C-O_B-M_D$	95.09(4)	94.97(5)	95.5(2)/96.4(2)
$M_C-O_D-M_D$	97.95(4)	97.27(6)	97.0(2)/97.1(2)
av. M−O−M (SF)	96.52	96.40	96.3/96.4
av. M−O−M (OF)	100.22	100.28	99.9/99.8

[a]See Figure 2 for numbering scheme.

The tetranuclear nature of **1** and **2** was also confirmed by positive ion electrospray ionization mass spectrometry (ESI-MS) in C_3H_6O or MeCN solution (Supporting Information, Figure S3), which in both cases showed a prominent peak at m/z = 1043 characteristic for the singly charged $[Ni_4L_4 + H]^+$ ion. This suggests that the cubane-type complexes are stable in solution, but readily loose their solvent ligands (MeOH or H_2O).

Magneto Structural Correlations for $\{Ni_4(\mu_3\text{-}O)_4\}$ Cubes. To better understand the magnetic properties of the new complexes **1** and **2** and to put them into broader perspective, we decided to undertake a thorough assessment of known magneto structural correlations for such type of compounds. Earlier studies of a number of complexes with distorted $\{Ni_4O_4\}$ cubane structures, whose exchange interactions are mediated only by μ_3-OR (R = H, Me) bridges, had suggested a linear correlation between the exchange coupling constant J and Ni−O−Ni_{av} bond angles: for Ni−O−Ni angles α below 99° the interaction was suggested to be ferromagnetic, and for α > 99° antiferromagnetic (Christou et al., 1995; Tuchagues et al., 2000).[20,21] However, in two more recent papers from 2007, where magnetic properties of 40[22] and 53[23] $\{Ni_4(\mu_3\text{-}OR)_4\}$ cubane structures were evaluated, it was concluded that a useful magnetostructural correlation is unlikely to be established for this type of complexes, since additional factors such as the identity of the capping ROH ligand would also influence intracluster magnetic exchange. Furthermore, the sign and magnitude of J were found to be sensitive even to slight distortions of the cubane core away from tetrahedral symmetry. To test these conclusions we analyzed the magnetic and structural parameters of some selected $\{Ni_4(\mu_3\text{-}OR)_4\}$ cubes that were already listed in the above-mentioned overviews, and also some more recent examples. To avoid any interference caused by additional magnetic exchange pathways, only complexes with exchange interactions mediated solely by μ_3-OR bridges, that is, without any secondary bridges like acetate spanning the nickel(II) ions, were taken into account. The results are summarized in Table 2.

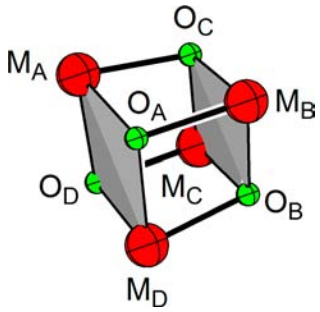

Figure 2. Emphasis of the cubane-like $\{Ni_4O_4\}$ fragment. Gray faces are not spanned by hydrogen bonds. $1\cdot H_2O$: M_A= Ni1, O_A = O2, M_B = Ni1′, O_B = O2′, M_C = Ni1″, O_C = O2″, M_D = Ni1‴, O_D = O2‴ ; $2\cdot 4C_3H_6O$: M_A = Ni1, O_A = O2, M_B = Ni2, O_B = O12, M_C = Ni2′, O_C = O12′, M_D = Ni1′, O_D = O2′ ; $2\cdot CH_2Cl_2$ (two crystallographically independent molecules): M_A = Ni1/5, O_A = O2/42, M_B = Ni2/6, O_B = O12/52, M_C = Ni3/7, O_C = O22/62, M_D = Ni4/8, O_D = O32/72. Symmetry operations used to generate equivalent atoms of $1\cdot H_2O$: (′) 1.25−y, 0.25+x, 1.25−z; (″) −0.25+y, 1.25−x, 1.25−z; (‴) 1−x, 1.5−y, z. Symmetry operation used to generate equivalent atoms of $2\cdot 4C_3H_6O$: (′) 1−x, y, 0.5−z.

Figure 3 shows a plot of the coupling constant J vs the (Ni−O−Ni)$_{av}$ angle α for the various complexes listed in Table 2.[36] At first sight it seems that indeed some points strongly deviate from the linear correlation. A more detailed inspection of the individual cases reveals, however, that all those outliers (reflected by open circles) feature particular situations that can readily explain their abnormal J values, without compromising the general validity of the linear correlation between J and α. (i) The small coupling constant J = −5.14 cm^{-1} for **H** despite its wide (Ni−O−Ni)$_{av}$ angle of 103.4° may be attributed to the different nature of the μ_3-OR bridge, namely, phenoxido, compared to alkoxido or hydroxido bridges in all other cases. (ii) Complex **F** was published twice, but with differing sets of magnetic parameters; one of them (**F1**)[28] fits well to the linear correlation, the other (**F2**)[16] does not, thus casting some doubt on the latter values. (iii) In the case of **J** the structure reveals two sets of structural parameters, but only a

dx.doi.org/10.1021/ic300535d | Inorg. Chem. 2012, 51, 8141−8149

Table 2. Literature Structural and Magnetic Data for Complexes with a $[Ni_4(\mu_3\text{-}OR)_4]^{4+}$ Cubane Core

complex	μ_3-OR	Ni−O−Ni$_{av}$ [deg]	J [cm^{-1}]	g	denotation[a] in [ref.]
A	methoxido	97.73	7.46	2.15	24
B	hydroxido	99.0	−0.57	2.20	25
C	methoxido	100.9	−9.1	2.00	26
D	hydroxido	95.85	17.5	2.0	27
	hydroxido	103.2	−22		
E	methoxido	96.7	12.2	2.05	**1** in [20]
	methoxido	99.6	−3.4		
F1	alkoxido	97.8[b]	5.28	2.11	**1** in [28]
	alkoxido	99.4[b]	0.43		
F2	alkoxido	97.8	2.75	2.06	**1** in [16]
	alkoxido	99.4	9.24		
G	alkoxido	97.26	7.29	2.15	[29]
	alkoxido	100.4	−2.08		
H	alkoxido	96.85	6.87	2.15	**2** in [30]
	alk./phen.	98.08	4.62		
	phenoxido	103.4	−5.14		
I	alkoxido	96.3	10.2	2.1	**1** in [31]
	alkoxido	98.15	2.4		
J	alkoxido	97.8	2.7	2.3	**2** in [32]
K	alkoxido	94.6	2.21	2.03	[33]
	alkoxido	101.6	−13.2		
L	alkoxido	96.1	7.15	2.14	[34]
	alkoxido	98.5	−0.34		
M	alkoxido	97.2	11.63	2.14	**1** in [35]
	alkoxido	100.3	1.38		

[a]If more than one compound. [b]Structural parameters taken from [16].

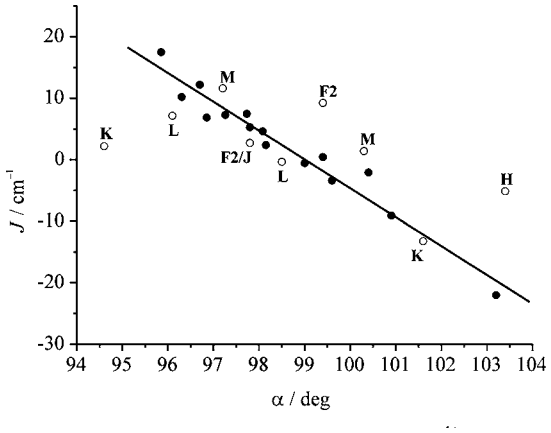

Figure 3. Effect of (Ni−O−Ni)$_{av}$ bond angle on J for $[Ni_4(\mu_3\text{-}OR)_4]^{4+}$ cubanes. Solid circles: literature data **A**–**I** (except data for **F2** and phenoxido bridged derivative of **H**) used for the linear fit (solid line). Open circles: data not included in the linear fit (see text).

single J in a simplified coupling scheme was used for magnetic data analysis.[32] (iv) Two coupling constants were used for fitting the magnetic properties of complex **K**,[33] though the structure clearly shows three distinct pathways. (v) In complex **L**[34] the used model does not properly reflect the core symmetry: similar faces of the cube are not opposite (as assumed according to the author's coupling scheme), but side by side. (vi) Complex **M**[35] was reported to feature ferromagnetic coupling (positive J) despite a wide angle α of 100.3°. We reinvestigated this case: we took the reported parameters (g, J_1, J_2), simulated the magnetic properties and then fitted the simulated curve. A fit of equal quality is also possible using other parameter sets including $J = -5$ cm^{-1} for the Ni−O−Ni fragment that has $\alpha = 100.3°$; the latter values nicely falls onto the solid correlation line in Figure 3.

All other examples (solid circles in Figure 3) are in good agreement with the linear correlation $J = -4.69\alpha + 464.4$ ($R^2 = 0.951$), which is comparable to the original correlation dating from 1995[20] with $J = -5.32\alpha + 566.7$ ($R^2 = 0.998$). Hence our conclusion from this analysis is that the correlation between the (Ni−O−Ni)$_{av}$ bond angle and J does exist and is clearly evident. Likely reasons for discrepancies in individual cases have been discussed above. For the present new complexes **1** and **2** we will examine in the following some further factors like the mutual dependence of the fit parameters J_i. Further the effect of exchanging exogenous ROH ligands at the $\{Ni_4(\mu_3\text{-}OR)_4\}$ core or removing lattice solvent molecules will be considered. It is shown that the identity of the exogenous ROH ligand and the presence of lattice solvent molecules strongly depend on experimental conditions (such as the time between isolation of the sample from its mother liquor and the actual measurement).

Magnetic Properties of $[Ni_4L_4(MeOH)_4]$ and $[Ni_4L_4(H_2O)_4]$. Magnetic susceptibility data were collected for complexes $[Ni_4L_4(MeOH)_4]\cdot H_2O$ (**1·H$_2$O**), $[Ni_4L_4(H_2O)_4]\cdot 4C_3H_6O$ (**2·4C$_3$H$_6$O**), and $[Ni_4L_4(H_2O)_4]\cdot H_2O$ (**2·H$_2$O**) in the temperature range from 295 to 2.0 K. No significant field dependence was observed when data were measured at applied fields of 0.2 and 0.5 T.

The initial investigation of **1·H$_2$O** revealed an unexpected aging effect, that is, the magnetic properties of freshly isolated material and of samples that were stored in air for some days were found to differ drastically. A series of additional magnetic measurements combined with elemental analyses, thermogravimetry, and meticulous synthetic work allowed explaining the initial observation. The product $\chi_M T$ of pristine **1·H$_2$O** increases gradually with decreasing temperature to reach a maximum of 9.19 cm^3 K mol^{-1} at 8 K (Figure 4, red circles).

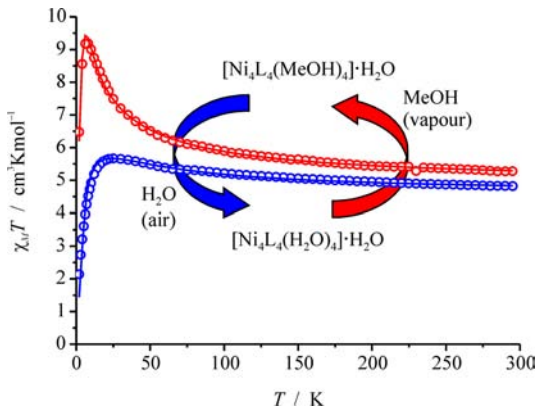

Figure 4. Plot of $\chi_M T$ versus temperature for **1·H$_2$O** (red open circles) and **2′·H$_2$O** (blue open circles) at 0.5 T. The solid lines represent the calculated curve fits.

Three days later, and after exposure to air, the same sample showed a maximal $\chi_M T$ value of only 5.67 cm^3 K mol^{-1} at 25 K (Figure 4, blue circles). The elemental analysis of the aged sample suggested that the exogenous MeOH ligands in $[Ni_4L_4(MeOH)_4]\cdot H_2O$ (**1·H$_2$O**) had been exchanged by H$_2$O molecules from aerial moisture to give $[Ni_4L_4(H_2O)_4]\cdot H_2O$ (**2′·H$_2$O**).[37] Ligand exchange is fully reversible: **2′·H$_2$O** can be

dx.doi.org/10.1021/ic300535d | Inorg. Chem. 2012, 51, 8141−8149

transformed back to **1′·H₂O** by exposing the crystals to MeOH vapor in a flask.[37] This reversible process is conveniently evidenced by repeated superconducting quantum interference device (SQUID) measurements, since the original $\chi_M T$ versus T curve is fully restored after exposure to MeOH, that is, **1·H₂O** and **1′·H₂O** have virtually identical magnetic properties.

Experimental magnetic data for all complexes were simulated using a fitting procedure to the appropriate Heisenberg–Dirac–van Vleck (HDvV) spin Hamiltonian for isotropic exchange coupling, Zeeman splitting, and zero field splitting (ZFS) (eq 1).[38]

$$\hat{H} = -2J_1(\hat{S}_1\hat{S}_2 + \hat{S}_1\hat{S}_3 + \hat{S}_2\hat{S}_4 + \hat{S}_3\hat{S}_4) - 2J_2(\hat{S}_2\hat{S}_3 + \hat{S}_1\hat{S}_4) + g\mu_B B\sum_{i=1}^{4}\hat{S}_{zi} + D\sum_{i=1}^{4}\left(\hat{S}_{iz}^2 - \hat{S}_i(\hat{S}_i+1)/3\right) \quad (1)$$

Parameter J_1 characterizes exchange across the four side faces (**SF**) of the $[Ni_4O_4]$ cube that are bridged by hydrogen bonds, while J_2 characterizes the remaining two opposite (**OF**, opposite faces) pair interactions (Scheme 2).

Scheme 2. Magnetic Coupling Scheme for All Complexes Reported in This Work[a]

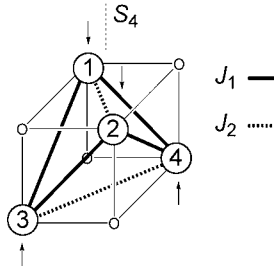

[a]Arrows indicate the distortion of the Ni_4 tetrahedron that results in S_4 symmetry, not spin alignment.

Taking **1·H₂O** as an example, the 3D error surface for the pairs J_1–J_2 shows that both parameters, J_1 and J_2, are almost linearly dependent (Figure 5); therefore the fitting does not lead to a unique solution.

For magnetic data analyses according to (eq 1) we thus decided to fix J_2 at the value calculated from the above magnetostructural correlation, using the angle α determined by X-ray analysis. In the case of **1·H₂O** this results in $J_2 = -5.63$ cm^{-1} for $\alpha = 100.22°$ (**OF**). The other coupling constant J_1 was then determined as +8.90 cm^{-1}, in reasonable agreement with the value of +11.72 cm^{-1} predicted from the magnetostructural correlation for $\alpha = 96.52°$ (**SF**). Parameters for **1·H₂O**, **2′·H₂O**, and **1′·H₂O** are collected in Table 3. In view of the linear dependence of J_1 and J_2 the ratio $|J_1/J_2|$ appears to be most significant. It is considerably higher for **1·H₂O** than for **2′·H₂O** (1.58 versus 1.27, Table 3). Noteworthy, for all complexes the best quality magnetic data simulation gave relatively large values of the axial single ion anisotropy parameter $|D| \approx 10$ cm^{-1}. Calculation of the 3D error surface for the pairs J_1–D (Supporting Information, Figure S4) revealed that these two parameters are independent and provide only one unique solution (if J_2 is fixed). Since the reliability of D values calculated from such powder susceptibility measurements is limited, magnetization measurements at variable temperature and variable field (VTVH) were performed for **1·H₂O** as a representative example (Supporting Information, Figure S5).

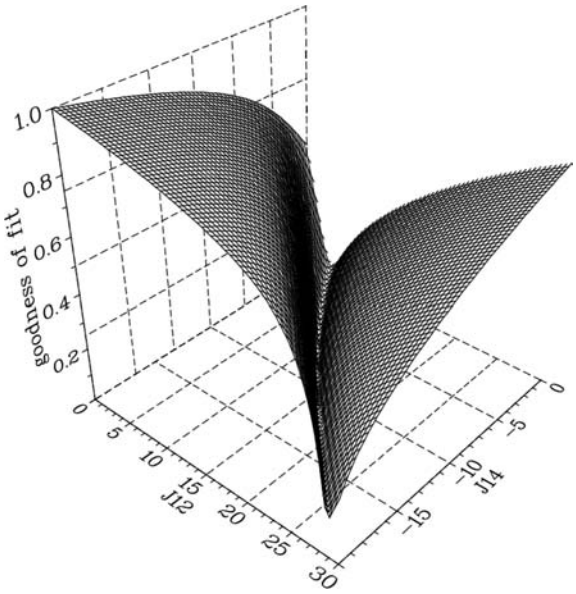

Figure 5. 3D error surface for the pairs $J_1(J_{12})$–$J_2(J_{14})$ for **1·H₂O**.

Isofield lines are not superimposable, confirming significant anisotropy of the ground state. Fit parameters for the VTVH data are in good agreement with those obtained from powder susceptibility measurements (see legend to Supporting Information, Figure S5), which supports the presence of large positive anisotropy values. It should be noted that the overall (molecular) ZFS is the tensorial sum of the single ion ZFS, and therefore the mutual compensation of single ion ZFS can lead to much smaller overall ZFS; in fact, values <1 cm^{-1} have previously been derived from HF-EPR measurements on some nickel cubane complexes.[29,39] The positive sign of D for **1·H₂O** explains the absence of any alternating current (AC) susceptibility signal that is typically observed for SMMs, since a negative D is required for this phenomenon.

It turns out that the different ratios $|J_1/J_2|$ for **1·H₂O** and **2′·H₂O** give rise to a dramatic change in the spin ground state, S_T, of the $[Ni_4O_4]$ cube. Both, the energy level calculation (see Supporting Information) and the simulation of $\chi_M T$ for given sets of J_1 and J_2 lead to $S_T = 4$ for **1·H₂O**, but $S_T = 0$ for **2′·H₂O** (neglecting any zero field splitting; Figure 6). Magnetization data of **1·H₂O** at 2 K (M versus H) give 7.9 $N\mu_B$ at 5 T, which is close to saturation for $S_T = 4$ and confirms the ferromagnetic ground state (Supporting Information, Figure S6). Interestingly, when keeping J_2 constant at −5.63 cm^{-1} a slight decrease of J_1 from +8.90 cm^{-1} to +8.30 cm^{-1}—which corresponds to a change of α of only 0.13°!—leads to switching of the ground state, namely, from a high-spin (ferromagnetic) ground state for $|J_1/J_2| > 1.5$ to a low-spin (diamagnetic) ground state for $|J_1/J_2| < 1.5$ (Figure 6). Such high sensitivity of the spin ground state toward subtle structural perturbations suggests that the switching of the spin ground state upon reversible interconversion of **1·H₂O** and **2′·H₂O** (see Figure 4) is caused by some minor structural rearrangement of the $[Ni_4O_4]$ core that is induced by the MeOH ↔ H_2O ligand exchange.

Since **2·4C₃H₆O** has four coordinated H_2O molecules, that is, a $[Ni_4L_4(H_2O)_4]$ core, one might expect that its magnetic properties should be similar to those of (i) **2′·H₂O** if the nature of coordinated solvent (H_2O versus MeOH) plays the crucial role or of (ii) **1·H₂O** if the geometrical parameters are more important. A SQUID measurement after standard workup

dx.doi.org/10.1021/ic300535d | Inorg. Chem. 2012, 51, 8141–8149

Table 3. Best Fit Parameters of Magnetic Data Analysis for Complexes Studied in This Work

complex	g	J_1 [cm^{-1}]	J_2 [cm^{-1}]	$\|D\|$ [cm^{-1}]	$\|J_1/J_2\|$	TIP [10^{-4} cm^{3}mol^{-1}]
1·H$_2$O	2.22	+8.90	−5.63 (fixed)	11.7	1.58	1.25
2′·H$_2$O	2.14	+7.17	−5.63 (fixed)	14.2	1.27	2.00 (fixed)
1′·H$_2$O	2.22	+8.86	−5.63 (fixed)	11.8	1.57	1.25 (fixed)
2·4C$_3$H$_6$O[a]	2.17	+8.90	−5.91 (fixed)	8.9	1.51	0.94 (fixed)
2·4C$_3$H$_6$O[b]	2.18	+8.25	−5.91 (fixed)	8.2	1.40	1.03 (fixed)
2·2C$_3$H$_6$O	2.20	+8.15	−5.91 (fixed)	11.0	1.38	1.49
2·H$_2$O	2.19	+4.43	−3.32	13.6	1.33	2.26

[a]Crystalline material measured in the range 2 K → 100 K. [b]Sample after warming to 295 K inside the SQUID magnetometer, measured in the range 295 K → 2 K.

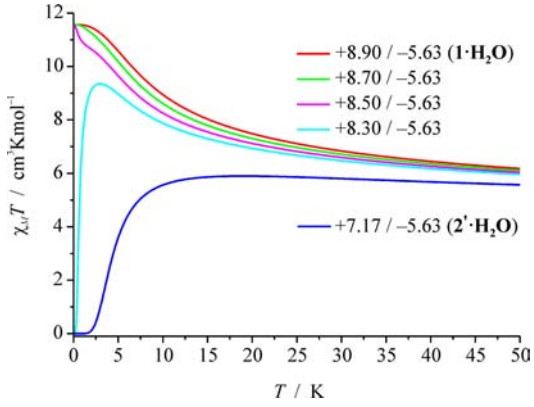

Figure 6. . Simulated $\chi_M T$ curves for [Ni$_4$O$_4$] cubes down to 0.1 K at 0.0001 T using g = 2.15 and different J_1 values at constant J_2 = −5.63 cm^{-1}.

procedure, that is, isolation of the crystalline sample, drying in air, powdering, weighting, and so forth, showed close similarity to the data obtained for **2′·H$_2$O** (Figure 7, blue circles).

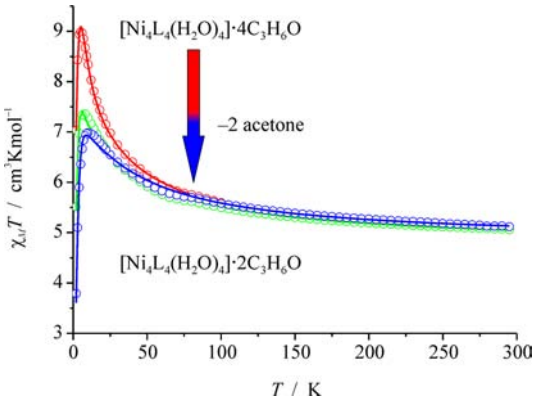

Figure 7. Plot of $\chi_M T$ versus temperature for **2·4C$_3$H$_6$O** at 0.5 T (2 K → 100 K; red open circles), the same sample at 0.2 T in cooling mode after warming to 295 K (295 K → 2 K; green open circles), and a dried powdered sample (**2·2C$_3$H$_6$O**) at 0.5 T (blue open circles). The solid lines represent the calculated curve fits.

However, an elemental analysis and thermogravimetry indicated that two of the four lattice acetone molecules had already been lost during workup of **2·4C$_3$H$_6$O**, suggesting that the resulting powder material is in fact **2·2C$_3$H$_6$O**. Interestingly, crystals that have been dried for only few minutes in air showed the same thermogravimetric properties as powdered samples that had been dried overnight: in both cases two of the four acetone molecules were rapidly lost already before the thermogravimetric measurement, while the remaining two acetone molecules are released from the lattice only by heating to above 370 K (Supporting Information, Figures S7 and S8); Ni-bound water ligands are lost at even higher temperatures above 400 K. This indicates that **2·2C$_3$H$_6$O** is in fact the form of this material that is investigated in all SQUID measurements once the sample has been dried, even for a short period. Subtle structural differences may well exist between the molecular entities in the powder and the crystal, for example, upon loss of lattice solvent such as the two acetone molecules from **2·4C$_3$H$_6$O**, which might have a substantial effect on the magnetic properties.[10] We therefore tried to measure the intact crystals of **2·4C$_3$H$_6$O** by directly immersing freshly isolated crystals together with some mother liquor in oil and rapidly freezing the sample inside of the SQUID magnetometer. Data measured from 2 to 100 K are shown as red circles in Figure 7.

Without removing the sample from the SQUID the same sample was then warmed up to 295 K and subsequently measured in cooling mode to 2 K (Figure 7, green circles). The $\chi_M T$ curve in cooling mode (295 to 2 K, green circles) is very similar to the curve for powdered **2·2C$_3$H$_6$O**, indicating that the reduced pressure in the sample space of the SQUID magnetometer is sufficient to remove at least partially the lattice solvent molecules from **2·4C$_3$H$_6$O** at ambient temperature. This evidently leads to significant changes of the magnetic properties. The analysis of all three data sets (for crystalline **2·4C$_3$H$_6$O**, for the same sample after warming to 295 K inside the SQUID, and for powdered **2·2C$_3$H$_6$O**) with J_2 fixed to −5.91 cm^{-1} (according to α = 100.28° for **OF**, derived from the crystallographic structure for **2·4C$_3$H$_6$O**) gave fit parameters that are collected in Table 3.

The ratio $|J_1/J_2|$ for pristine **2·4C$_3$H$_6$O** is 1.51 and slightly higher than the critical value of 1.5; thus, the ground state should be ferromagnetic; this is confirmed by the energy level calculation (see Supporting Information). However, the ground state S_T = 4 is only about 0.3 cm^{-1} lower than the first excited state S = 0. For **2·2C$_3$H$_6$O** the order of those energy levels becomes inverted, that is, S_T = 0 now is the ground state, with an energy separation of 5.7 cm^{-1}. The finding that the calculated ratio $|J_1/J_2|$ for **2·4C$_3$H$_6$O** (1.51, which is a borderline case between magnetic and nonmagnetic ground states) is still lower than $|J_1/J_2|$ for **1·H$_2$O** (1.58) despite structural similarity might be due to exiguous release of some acetone molecules from the crystal before starting the SQUID data collection, despite careful preparation of the sample.

Further attempts to crystallize the complex [Ni$_4$L$_4$(H$_2$O)$_4$] led to **2·CH$_2$Cl$_2$** ([Ni$_4$L$_4$(H$_2$O)$_4$]·CH$_2$Cl$_2$) and **2·H$_2$O** ([Ni$_4$L$_4$(H$_2$O)$_4$]·H$_2$O). The complex **2·CH$_2$Cl$_2$** is structurally similar to **2·4C$_3$H$_6$O** and again has a volatile solvent molecule included in the crystal lattice that hampers SQUID measure-

dx.doi.org/10.1021/ic300535d | Inorg. Chem. 2012, 51, 8141−8149

ments of a pristine sample. Crystals of **2·H$_2$O** have the same composition as **2′·H$_2$O** (which results from **1·H$_2$O** after exchange of coordinated solvent MeOH → H$_2$O), and therefore this material is an excellent candidate for corroborating the ideas for the various transformations discussed above. Indeed, the magnetic parameters for **2·H$_2$O** (Figure 8, Table 3) are very similar to those of **2′·H$_2$O** (Figure 8).

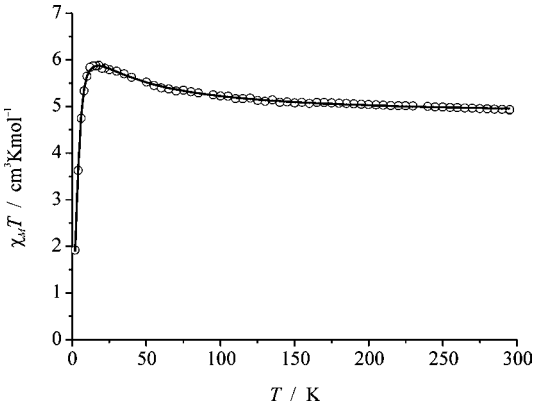

Figure 8. Plot of $\chi_M T$ versus temperature for **2·H$_2$O** at 0.5 T. The solid line represents the calculated curve fit.

Unfortunately, the quality of the X-ray crystallographic structure determination of **2·H$_2$O** (Supporting Information, Figure S1b) is moderate and does not allow any detailed magnetostructural analysis or discussion of atom distances and bond angles. However, the fact that **2′·H$_2$O** and **2·H$_2$O** have very similar magnetic properties and the same composition supports the conclusion that the geometrical parameters of **1·H$_2$O** undergo changes upon solvent exchange, which has a critical influence on the ground state of the [Ni$_4$O$_4$] cubes.

CONCLUSIONS

In this paper we have described a series of new alkoxo-bridged tetranuclear Ni^{II} cube structures. The reversible exchange in the solid state of the coordinated solvent between [Ni$_4$L$_4$(MeOH)$_4$]·H$_2$O (**1·H$_2$O**) and [Ni$_4$L$_4$(H$_2$O)$_4$]·H$_2$O (**2′·H$_2$O**) goes along with a switching of the spin ground state from S_T = 4 to S_T = 0. Likewise the (irreversible) loss of lattice solvent in [Ni$_4$L$_4$(H$_2$O)$_4$]·4C$_3$H$_6$O (**2·4C$_3$H$_6$O**) to give **2·2C$_3$H$_6$O** changes the ground state from magnetic (S_T = 4) to diamagnetic (S_T = 0). Both processes − reversible exchange of the coordinated solvent in **1·H$_2$O** and the loss of lattice solvent in **2·4C$_3$H$_6$O** − are accompanied by slight structural rearrangements of the [Ni$_4$O$_4$] core, which results in drastic changes of the magnetic properties. The conclusions from this work can be summarized as follows.

(i) A correlation between the (Ni−O−Ni)$_{av}$ bond angle and J in [Ni$_4$O$_4$] cubane complexes does indeed exist.

(ii) Minor structural perturbations (such as changes of Ni−O−Ni angles) in such cubes can give rise to drastic differences in the magnetic properties, namely a switching of the spin ground state between S_T = 4 and S_T = 0.

(iii) The [Ni$_4$O$_4$] cube in the present complexes is a robust core that allows facile and reversible exchange of exogenous solvent ligands.

(iv) Great caution is advisable when interpreting magnetic data obtained for powdered material or for crystals that easily loose lattice solvent molecules under reduced pressure (such as in the sample chamber of the SQUID magnetometer), since this may lead to minor structural rearrangements that yet cause drastic changes in the magnetic properties. Since crystallographic analyses obtained for molecular compounds in most cases show the presence of volatile solvent molecules in the crystal lattice, any magnetic data interpretation and magnetostructural correlation that relies on geometric parameters for the pristine crystal requires careful evaluation of the effect of sample treatment for magnetic measurements.

Studies on further cubane-type complexes with H$_2$L and related ligands, including metals such as Co^{II} and Fe^{II}, are ongoing in our laboratory.

EXPERIMENTAL SECTION

Materials and Methods. Solvents were purified by established procedures.[40] All other chemicals were purchased from commercial sources and used as received. Microanalyses were performed by the Analytical Laboratory of the Institute of Inorganic Chemistry at Georg-August-University Göttingen using an Elementar Vario EL III. IR spectra were recorded using a Digilab Excalibur Series FTS 3000 spectrometer at room temperature. Mass spectra were measured using a Finnigan MAT LCQ mass spectrometer (ESI-MS). Thermogravimetric measurements were performed using a Netzsch STA409PC LUXX, scan rate: 5 K/min. Magnetic data were measured with a Quantum-Design MPMS-XL-5 SQUID magnetometer equipped with a 5 T magnet in the range from 2 to 295 K. Samples were treated as described in the main section of this manuscript, then contained in a gel bucket, and fixed in a nonmagnetic sample holder. Each raw data file for the measured magnetic moment was corrected for the diamagnetic contribution of the sample holder and the sample. A Curie-behaved paramagnetic impurity (PI) with spin S = 1 (fixed to 0.1%) and temperature-independent paramagnetism (TIP) were included according to χ_{calc} = (1 − PI)·χ + PI·χ_{mono} + TIP. Before simulation, the experimental data were corrected for TIP.

Synthesis of [Ni$_4$(MeOH)$_4$(L)$_4$]·H$_2$O (1·H$_2$O). Ni(OAc)$_2$·4H$_2$O (305 mg, 1.22 mmol) was added to a solution of H$_2$L (250 mg, 1.22 mmol) in methanol (50 mL), and then NaOH (98 mg, 2.44 mmol) in methanol (10 mL) was added dropwise to the reaction mixture, affording a green precipitate almost immediately. The green precipitate was collected by filtration, washed with methanol, and dried in air. The resulting green powder was then dissolved in CH$_2$Cl$_2$ (50 mL) and layered with *n*-hexane. Green crystals of **1·H$_2$O** were separated after several days. Yield: 80 mg (22%). MS (ESI, C$_3$H$_6$O): *m*/*z* (%), 1043 (30), [L$_4$Ni$_4$+ H]$^+$; 1064.9 (20), [L$_4$Ni$_4$+ Na]$^+$. IR (KBr): $\tilde{\nu}$ 3340 (br), 3045 (w), 2926 (w), 2866 (w), 2766 (w), 1597 (s), 1556 (s), 1518 (m), 1498 (m), 1466 (s), 1441 (m), 1415 (w), 1371 (w), 1317 (s), 1352 (m), 1211 (w), 1191 (w), 1130 (s), 1110 (w), 1070 (s), 1035 (w), 955 (w), 886 (m), 847 (m), 770 (w), 747 (s), 690 (w), 611 (w) cm^{-1}. Elemental analysis (%) calculated for C$_{48}$H$_{58}$Ni$_4$N$_8$O$_{13}$ (1189.8): C, 48.45; H, 4.91; N, 9.42. Found: C, 48.05; H, 4.71; N, 9.57.

Synthesis of [Ni$_4$L$_4$(H$_2$O)$_4$]·4C$_3$H$_6$O (2·4C$_3$H$_6$O). The crude material was synthesized as described above for **1·H$_2$O**. After filtration the resulting green powder was dissolved in acetone (60 mL) and the solution left for slow evaporation of the solvent. Green crystals of the product **2·4C$_3$H$_6$O** formed within several days. After separation from the mother liquor the crystals show rapid loss of solvent molecules; the composition of the air-dried compound [Ni$_4$L$_4$(H$_2$O)$_4$]·2C$_3$H$_6$O was determined by elemental and thermogravimetric analysis. Thermogravimetry of powdered crystals of **2·4C$_3$H$_6$O** dried overnight showed the stepwise loss of solvent molecules: two acetone molecules were already lost before the measurement, two acetone molecules are lost until 405 K is reached (mass loss: exp. 9.9%, calc. 9.4%) and four water molecules are finally lost in the range 405−500 K (mass loss: exp. 5.5%, calc. 5.8%). MS (ESI, MeCN): *m*/*z* (%), 1043 (62), [L$_4$Ni$_4$+H]$^+$, 522 (25), [L$_4$Ni$_4$+2H]$^{2+}$. IR (KBr): $\tilde{\nu}$ 3570 (w), 3445 (br), 3044 (w), 3020 (w), 2934 (br), 2868 (w), 1695 (m), 1597 (s), 1555 (m), 1520 (s), 1499 (s), 1467 (s), 1441 (s), 1411 (w), 1368 (w), 1354 (w), 1323 (vs), 1258 (m), 1229 (w), 1206 (w), 1130 (m), 1092

dx.doi.org/10.1021/ic300535d | Inorg. Chem. 2012, 51, 8141−8149

Table 4. Crystal Data and Refinement Details for $1{\cdot}H_2O$, $2{\cdot}4C_3H_6O$, and $2{\cdot}CH_2Cl_2$

	$1{\cdot}H_2O$	$2{\cdot}4C_3H_6O$	$2{\cdot}CH_2Cl_2$
empirical formula	$C_{48}H_{56}N_8Ni_4O_{13}$	$C_{56}H_{72}N_8Ni_4O_{16}$	$C_{90}H_{84}Cl_4N_{16}Ni_8O_{24}$
formula weight	1187.85	1348.06	2385.21
crystal size [mm^3]	0.42 × 0.21 × 0.07	0.37 × 0.26 × 0.23	0.50 × 0.13 × 0.05
crystal system	tetragonal	monoclinic	orthorhombic
space group	$I4_1/a$	$P2/c$	$Fdd2$
a [Å]	16.8120(7)	9.2598(3)	45.9586(2)
b [Å]	16.8120(7)	11.9585(2)	96.6583(12)
c [Å]	17.5449(9)	26.1511(7)	8.463(2)
α [deg]	90.00	90.00	90.00
β [deg]	90.00	90.022(2)	90.00
γ [deg]	90.00	90.00	90.00
V [Å^3]	4958.9(4)	2895.80(13)	37594(11)
Z	4	2	16
ρ [g/cm^3]	1.591	1.546	1.686
$F(000)$	2464	1408	19520
μ [mm^{-1}]	1.569	1.357	1.764
T_{min}/ T_{max}	0.6923/0.8420	0.6405/0.7673	0.5587/0.8657
θ range [deg]	1.68−27.15	1.70−25.63	1.22−24.60
hkl range	±21, ±21, ±22	−11 to 9, ±14, ±31	±53, −111 to 112, −9 to 8
measured refl.	44432	29973	56600
unique refl. [R_{int}]	44432 [0]	5462 [0.0407]	14003 [0.1076]
observed refl. ($I > 2\sigma(I)$)	23704	5388	10027
data/restraints/param.	44432/418/229	5462/4/392	14003/259/1335
goodness-of-fit (F^2)	1.012	1.085	1.006
$R1$, $wR2$ ($I > 2\sigma(I)$)	0.0622, 0.1373	0.0226, 0.0595	0.0509, 0.0787
$R1$, $wR2$ (all data)	0.1179, 0.1540	0.0231, 0.0597	0.0792, 0.0842
resid. el. dens. [e/Å^3]	−0.422/0.705	−0.370/0.588	−0.518/0.488

(m), 1072 (m), 958 (w), 886 (m), 849 (m), 748 (s), 688 (w), 644 (w), 612 (w), 571 (m), 554 (m), 452 (m) cm^{-1}. Elemental analysis (%) calculated for $C_{50}H_{60}Ni_4N_8O_{14}$ (1231.8): C, 48.75; H, 4.90; N, 9.10. Found: C, 48.03; H, 4.82; N, 9.01.

Synthesis of $[Ni_4L_4(H_2O)_4]{\cdot}CH_2Cl_2$ ($2{\cdot}CH_2Cl_2$) and Synthesis of $[Ni_4L_4(H_2O)_4]{\cdot}H_2O$ ($2{\cdot}H_2O$). The crude material was synthesized as described above for $1{\cdot}H_2O$, but using slightly moist solvents. The green precipitate was collected by filtration, washed with methanol, and dried in air. Both compounds were crystallized simultaneously upon dissolving the green powder in CH_2Cl_2 (50 mL), followed by layering with *n*-hexane. For $2{\cdot}CH_2Cl_2$ the crystals were suitable for X-ray diffraction; in case of $2{\cdot}H_2O$ a crystal structure determination confirmed the proposed molecular structure, but was of moderate quality. Magnetic susceptibility data were measured for some carefully selected and separated crystals of $2{\cdot}H_2O$, but no further characterization of both compounds was attempted because of the formation of a mixture of both and low yields of crystalline material.

X-ray Crystallography. Crystal data and details of the data collections are given in Table 4. X-ray data were collected on a STOE IPDS II diffractometer (graphite monochromated Mo−Kα radiation, λ = 0.71073 Å) by use of ω scans at −140 °C. The structures were solved by direct methods and refined on F^2 using all reflections with SHELX-97.[41] The non-hydrogen atoms were refined anisotropically. Most hydrogen atoms were placed in calculated positions and assigned to an isotropic displacement parameter of 1.2/1.5 U_{eq}(C). The positional parameters of the oxygen bound hydrogen atoms were refined by using DFIX restraints (d_{O-H} = 0.82 Å) in case of $2{\cdot}4C_3H_6O$ and without using a DFIX restraint in case of $1{\cdot}H_2O$. A fixed isotropic displacement parameter of 0.08 Å^2 was assigned to those hydrogen atoms. Hydrogen atoms of the disordered water molecule in **1** (fixed occupancy factor 0.25) and all oxygen bound hydrogen atoms in $2{\cdot}CH_2Cl_2$ could not be located. Parts of the ligands in $1{\cdot}H_2O$ (C1A/B−C9A/B) and $2{\cdot}CH_2Cl_2$ (C57A/B, C58A/B, C59A/B, C68A/B, C69A/B, C70A/B) were found to be disordered about two positions (occupancy factors $1{\cdot}H_2O$: 0.475(11)/ 0.525(11); $2{\cdot}CH_2Cl_2$: 0.54(2)/0.46(2) and 0.48(2)/0.52(2)). SAME, SADI, SIMU, DELU, and ISOR restraints were used to model the disorder. Crystals under investigation were found to be twinned in case of $2{\cdot}4C_3H_6O$ (twin law: 1 0 0, 0 −1 0, 0 0 −1; twin ratio 0.418(1): 0.582(1)) and $1{\cdot}H_2O$ (twin law: 0 −1 0, 0.05 0 −0.96, 1.04 0 0.5; twin ratio 0.297(1): 0.703(1)). For the latter a HKLF 5 format file was used for the refinement of the structure. The absolute structure parameter for $2{\cdot}CH_2Cl_2$, −0.002(13), was determined with SHELXL-97 according to Flack.[42] Face-indexed absorption corrections were performed numerically with the program X-RED.[43]

■ ASSOCIATED CONTENT

Ⓢ Supporting Information

Crystallographic data in CIF format. Further details are given in Figures S1−S14 and Tables S1−S7. This material is available free of charge via the Internet at http://pubs.acs.org.

■ AUTHOR INFORMATION

Corresponding Author

*Phone: +49 551 393012. Fax: +49 551 393063. E-mail: franc.meyer@chemie.uni-goettingen.de.

Notes

The authors declare no competing financial interest.

■ ACKNOWLEDGMENTS

Financial support by the DFG (SFB 602, project A16) is gratefully acknowledged.

■ REFERENCES

(1) Kahn, O.; Larionova, J.; Yakhmi, J. V. *Chem.—Eur. J.* **1999**, *5*, 3443−3449.

(2) Sato, Y.; Ohkoshi, S.; Arai, K.; Tozawa, M.; Hashimoto, K. *J. Am. Chem. Soc.* **2003**, *125*, 14590−14595.

(3) (a) Kepert, C. J. *Chem. Commun.* **2006**, 695−700. (b) Ferrando-Soria, J.; Ruiz-García, R.; Cano, J.; Stiriba, S.-E.; Vallejo, J.; Castro, I.; Julve, M.; Lloret, F.; Amorós, P.; Pasán, J.; Ruiz-Pérez, C.; Journaux, Y.; Pardo, E. *Chem.—Eur. J.* **2012**, *6*, 1608−1617.
(4) Liu, C.-M.; Zhang, D.-Q.; Zhu, D.-B. *Chem. Commun.* **2008**, 368−370.
(5) (a) Kurmoo, M.; Kumagai, H.; Chapman, K. W.; Kepert, C. J. *Chem. Commun.* **2005**, 3012−3014. (b) Zeng, M.-H.; Feng, X.-L.; Zhang, W.-X.; Chen, X.-M. *Dalton Trans.* **2006**, 5294−5303. (c) Nowicka, B.; Rams, M.; Stadnicka, K.; Sieklucka, B. *Inorg. Chem.* **2007**, *46*, 8123−8125. (d) Cheng, X.-N.; Zhang, W.-X.; Chen, X.-M. *J. Am. Chem. Soc.* **2007**, *129*, 15738−15739. (e) Zhao, J.-P.; Hu, B.-W.; Yang, Q.; Hu, T.-L.; Bu, X.-H. *Inorg. Chem.* **2009**, *48*, 7111−7116. (f) Zhang, Y.-J.; Liu, T.; Kanegawa, S.; Sato, O. *J. Am. Chem. Soc.* **2009**, *131*, 7942−7943.
(6) Hao, Z.-M.; Zhang, X.-M. *Dalton Trans.* **2011**, 2092−2098 , and references therein.
(7) (a) Dechambenoit, P.; Long, J. R. *Chem. Soc. Rev.* **2011**, *40*, 3249−3265. (b) Muñoz-Lara, F. J.; Gaspar, A. B.; Muñoz, M. C.; Arai, M.; Kitagawa, S.; Ohba, M.; Real, J. A. *Chem.—Eur. J.* **2012**, *18*, 8013−1018.
(8) Song, Y.-M.; Luo, F.; Luo, M.-B.; Liao, Z.-W.; Sun, G.-M.; Tian, X.-Z.; Zhu, Y.; Yuan, Z.-J.; Liu, S.-J.; Xu, W.-Y.; Feng, X.-F. *Chem. Commun.* **2012**, *48*, 1006−1008.
(9) (a) Motreff, A.; Correa da Costa, R.; Allouchi, H.; Duttine, M.; Mathonière, C.; Duboc, C.; Vincent, J.-M. *Inorg. Chem.* **2009**, *48*, 5623−5625. (b) Motreff, A.; Correa da Costa, R.; Allouchi, H.; Duttine, M.; Mathonière, C.; Duboc, C.; Vincent, J.-M. *J. Fluorine Chem.* **2012**, *134*, 49−55.
(10) Demeshko, S.; Leibeling, G.; Dechert, S.; Meyer, F. *Dalton Trans.* **2006**, 3458−3465.
(11) (a) Halder, G. J.; Kepert, C. J.; Moubaraki, B.; Murray, K. S.; Cashion, J. D. *Science* **2002**, *298*, 1762−1765. (b) Hostettler, M.; Törnroos, K. W.; Chernyshov, D.; Vangdal, B.; Bürgi, H.-B. *Angew. Chem., Int. Ed.* **2004**, *43*, 4589−4594. (c) Halcrow, M. A. *Coord. Chem. Rev.* **2009**, *253*, 2493−2514. (d) Chuang, Y.-C.; Liu, C.-T.; Sheu, C.-F.; Ho, W.-L.; Lee, G.-H.; Wang, C.-C.; Wang, Y. *Inorg. Chem.* **2012**, *51*, 4663−4671.
(12) Venkateswara Rao, P.; Holm, R. H. *Chem. Rev.* **2004**, *104*, 527−559.
(13) (a) Swiegers, G. F.; Clegg, J. F.; Stranger, R. *Chem. Sci.* **2011**, *2*, 2254−2262. (b) Dismukes, G. C.; Brimblecombe, R.; Felton, G. A. N.; Pryadun, R. S.; Sheats, J. E.; Spiccia, L.; Swiegers, G. F. *Acc. Chem. Res.* **2009**, *42*, 1935−1943.
(14) Shiga, T.; Oshio, H. *Sci. Technol. Adv. Mater.* **2005**, *6*, 565−570.
(15) Yang, E.-C.; Wernsdorfer, W.; Hill, S.; Edwards, R. S.; Nakano, M.; Maccagnano, S.; Zakharov, L. N.; Rheingold, A. L.; Christou, G.; Hendrickson, D. N. *Polyhedron* **2003**, *22*, 1727−1733.
(16) Yang, E.-C.; Wernsdorfer, W.; Zakharov, L. N.; Karaki, Y.; Yamaguchi, A.; Isidro, R. M.; Lu, G.-D.; Wilson, S. A.; Rheingold, A. L.; Ishimoto, H.; Hendrickson, D. N. *Inorg. Chem.* **2006**, *45*, 529−546.
(17) Moragues-Canovas, M.; Helliwell, M.; Ricard, L.; Riviere, E.; Wernsdorfer, W.; Brechin, E.; Mallah, T. *Eur. J. Inorg. Chem.* **2004**, 2219−2222.
(18) Das, A.; Gieb, K.; Krupskaya, Y.; Demeshko, S.; Dechert, S.; Klingeler, R.; Kataev, V.; Büchner, B.; Müller, P.; Meyer, F. *J. Am. Chem. Soc.* **2011**, *133*, 3433−3443.
(19) (a) Boskovic, C.; Rusanov, E.; Stoeckli-Evans, H.; Güdel, H. U. *Inorg. Chem. Commun.* **2002**, *5*, 881−886. (b) Hoshino, N.; Ito, T.; Nihei, M.; Oshio, H. *Chem. Lett.* **2002**, 844−845. (c) Sieber, A.; Boskovic, C.; Bircher, R.; Waldmann, O.; Ochsenbein, S. T.; Chaboussant, G.; Güdel, H. U.; Kirchner, N.; van Slageren, J.; Wernsdorfer, W.; Neels, A.; Stoeckli-Evans, H.; Janssen, S.; Juranyi, F.; Mutka, H. *Inorg. Chem.* **2005**, *44*, 4315−4325.
(20) Halcrow, M. A.; Sun, J. S.; Huffman, J. C.; Christou, G. *Inorg. Chem.* **1995**, *34*, 4167−4177.
(21) Clemente-Juan, J. M.; Chansou, B.; Donnadieu, B.; Tuchagues, J. P. *Inorg. Chem.* **2000**, *39*, 5515−5519.
(22) Isele, K.; Gigon, F.; Williams, A. F.; Bernardinelli, G.; Franz, P.; Decurtins, S. *Dalton Trans.* **2007**, 332−341.
(23) Wikstrom, J. P.; Nazarenko, A. Y.; Reiff, W. M.; Rybak-Akimova, E. V. *Inorg. Chim. Acta* **2007**, *360*, 3733−3740.
(24) (a) Andrew, J. E.; Blake., A. B. *J. Chem. Soc. A* **1969**, 1456−1461. (b) Barnes, J. A.; Hatfield, W. E. *Inorg. Chem.* **1971**, *10*, 2355−2357.
(25) (a) Aurivillius, B. *Acta Chem. Scand., Ser. A* **1977**, *31*, 501−508. (b) Boyd., P. D. W.; Martin, R. L.; Schwarzenbach, G. *Aust. J. Chem.* **1988**, *41*, 1449−1456.
(26) Gladfelter, W. L.; Lynch, M. W.; Schaefer, W. P.; Hendrickson., D. N.; Gray, H. B. *Inorg. Chem.* **1981**, *20*, 2390−2397.
(27) Ballester, L.; Coronado, E.; Gutiérrez, A.; Monge, A.; Perpiñán, M. F.; Pinilla, E.; Rico, T. *Inorg. Chem.* **1992**, *31*, 2053−2056.
(28) Escuera, A.; Font-Bardía, M.; Kumar, S. B.; Solans, X.; Vicente, R. *Polyhedron* **1999**, *18*, 909−914.
(29) Ferguson, A.; Lawrence, J.; Parkin, A.; Sanchez-Benitez, J.; Kamenev, K. V.; Brechin, E. K.; Wernsdorfer, W.; Hill., S.; Murrie, M. *Dalton Trans.* **2008**, 6409−6414.
(30) Hazra, S.; Koner, R.; Lemoine, P.; Sañudo, E. C.; Mohanta, S. *Eur. J. Inorg. Chem.* **2009**, 3458−3466.
(31) Ferguson, A.; Schmidtmann, M.; Brechin, E. K.; Murrie, M. *Dalton Trans.* **2011**, 334−336.
(32) Diewald, S.; Lan, Y.; Clérac, R.; Powell, A.-K.; Feldmann, C. *Z. Anorg. Allg. Chem.* **2008**, *634*, 1880−1886.
(33) Efthymiou, C. G.; Papatriantafyllopoulou, C.; Aromi, G.; Teat, S. J.; Christou, G.; Perlepes, S. P. *Polyhedron* **2011**, *30*, 3022−3025.
(34) Liang, Q.; Huang, R.; Chen, X.; Li, Z.; Zhang, X.; Sun, B. *Inorg. Chem. Commun.* **2010**, *13*, 1134−1136.
(35) Sun, J.-P.; Li, L.-C.; Zheng, X.-Y. *Inorg. Chem. Commun.* **2011**, *14*, 877−881.
(36) All J values have been adapted to the spin Hamiltonian defined as $H = -2J(S_1S_2)$ if necessary.
(37) **2′**·represents $[Ni_4L_4(H_2O)_4]$ obtained by ligand exchange from $[Ni_4L_4(MeOH)_4]$ (**1**). **1′** represents $[Ni_4L_4(MeOH)_4]$ obtained by ligand exchange from $[Ni_4L_4(H_2O)_4]$ (**2′**).
(38) Full-matrix diagonalization of exchange coupling and Zeeman splitting was performed with the julX program (E. Bill, Max Planck Institute for Bioinorganic Chemistry, Mülheim/Ruhr, Germany).
(39) (a) Lawrence, J.; Yang, E.-C.; Edwards, R.; Olmstead, M. M.; Ramsey, C.; Dalal, N. S.; Gantzel, P. K.; Hill, S.; Hendrickson, D. N. *Inorg. Chem.* **2008**, *47*, 1965−1974. (b) Aromí, G.; Bouwman, E.; Burzurí, E.; Carbonera, C.; Krzystek, J.; Luis, F.; Schlegel, C.; van Slageren, J.; Tanase, S.; Teat, S. J. *Chem.—Eur. J.* **2008**, *14*, 11158−11166.
(40) Becker, H. G. O.; Berger, W.; Domschke, G.; Fanghänel, E.; Faust, J.; Fischer, M.; Gentz, F.; Gewald, K.; Gluch, R.; Mayer, R.; Müller, K.; Pavel, D.; Schmidt, H.; Schollberg, K.; Schwetlick, K.; Seiler, E.; Zeppenfeld, G. *Organikum*, 19nd ed.; Johann Ambrosius Barth Verlag GmbH: Leipzig, Germany, 1993; p 668 ff.
(41) Sheldrick, G. M. *Acta Crystallogr.* **2008**, *A64*, 112−122.
(42) Flack, H. D. *Acta Crystallogr.* **1983**, *A39*, 876−881.
(43) *X-RED*; STOE & CIE GmbH: Darmstadt, Germany, 2002.